14th IEA Heat Pump Conference
15-18 May 2023, Chicago, Illinois

Investigation of a Novel Hybrid Heat Pump Concept

Tobias Reum*, David Schmitt, Thorsten Summ, Tobias Schrag

Institute for new Energy Systems (InES), Technische Hochschule Ingolstadt, Germany

Abstract

Hybrid heat pumps can utilize two low-grade ambient heat sources to provide heating energy. However, efficient operation of two heat sources and its effect on heat source dimensioning has not been thoroughly examined. In this research, a hybrid heat pump is developed which can switch between an air heat exchanger and a ground source heat exchanger as the heat source. The hybrid heat pump interconnection also allows parallel operation of both heat sources. Based on an experimental investigation, a black box model is created including a suitable control strategy. An annual simulation for space heating of a domestic building is conducted. The hybrid heat pump provides about 18.9 MWh of heat while extracting only 47.1 % of this heat from the ground source heat exchanger. Parallel operation allows a heating capacity reduction of the ground source heat exchanger to about 80 % compared to a conventional ground source heat pump. The hybrid heat pump therefore allows a smaller design size.

Selection and/or peer-review under the responsibility of the organizers of the 14th IEA Heat Pump Conference 2023.

Keywords: hybrid heat pump; dual source heat pump; parallel operation; black box model; annual simulation

1. Introduction

1.1. Background and motivation

Heat pumps are one of the main heat generators for future heating systems. The heat pump market is growing rapidly. In 2021, the heat pump sales in Germany grew by about 28 % [1], even before the current energy crisis in Europe. Heat pumps are expected to become a main heat generator in the domestic sector [2].

Heat pumps provide heat using highly efficient refrigerant cycles, operating as reverse Carnot engines [3]. A small amount of (usually electrical) work is needed to provide a large amount of heat. Heat pumps therefore enable a transition of the heat generation into a fully electrical system. Electricity can be provided by renewable energy sources, e.g. wind power and photovoltaics. The remaining heat is drawn from ambient low-grade reservoirs. This means they are also significantly more efficient than direct electric heaters for domestic purposes. The fraction between the delivered heat capacity $\dot{Q}_{heat}$ and the necessary electrical power P_{el} is called the coefficient of performance (COP):

$$\mathrm{COP} = \frac{\dot{Q}_{heat}}{P_{el}} \tag{1}$$

In practice, the COP usually varies between 2 and 6 depending on the temperature above levels of the ambient reservoir and the temperature needed for the heating system [4, 5]. This requires proper

* Corresponding author. Tel.: +49-841-9348-6841; fax: +49-0841-9348-996841.
E-mail address: tobias.reum@thi.de.

implementation into the buildings for high efficiencies, for example by adding thermal insulation or large area heating systems like floor heating. Common ambient heat reservoirs serving as the heat source are air, the soil and ground water. While air source heat pumps are relatively cheap and easy to install, the efficiency especially during peak heating load hours in winter is lacking due to low ambient (outside air) temperatures. Using the soil or ground water as the heat source promises higher efficiencies due to higher reservoir temperatures during winter months, but the installation costs for either heat source are usually higher and there are higher geological requirements. Ground water needs careful examination of the underground water flow. Using the soil with vertical boreholes demands geological investigations and often longer time scales due to bureaucratic allowances, while horizontal heat exchangers occupy large areas, which are an issue especially in urban spaces. Each heat source for heat pumps therefore has their own advantages and disadvantages.

1.2. Hybrid heat pumps

Hybrid heat pumps (HHPs) – in literature often also referred to as dual source heat pumps to not confuse these systems with systems combining a heat pump with a gas boiler – combine several ambient heat sources to utilize the aforementioned advantages while minimizing the disadvantages. Commonly, HHPs optimize the usage of the heat sources to increase either the efficiency of the system, to reduce the energy extracted from the secondary (commonly the ground) heat source to limit ground source heat exchanger (GSHX) size or to profit from both benefits.

Allaerts et al. [6] combined two borehole GSHX with an air-based regenerator. The system was designed for an office building, where the cooling load was the dominating requirement. The HHP operated with one of the GSHXs while the other could be regenerated passively (i.e., not using the refrigerant cycle) over the ambient air. Serially, the HHP operated either in heating mode or cooling mode with one of the GSHXs. They researchers still found that a decrease of about 47 % in borehole sizing was possible due to regeneration with this air-based regenerator as compared to a single ground-source heat pump system.

Another project by Cannistraro et al. [7] extended an existing air-to-air heat pump into a HHP for an air-conditioning system. The heat pump could utilize either an air source or a flat-plate GSHX to provide heating and cooling. During cold ambient air conditions, the HHP used the GSHX to provide heating. A mixed operation was possible without stating further details. They found an improved efficiency compared to the original air-to-air heat pump at specific operating conditions No annual comparison was given.

In a simulation-based study, Dongellini et al. [8] attempted to reduce the sizing for the borehole GSHX of an HHP. This HHP could also switch between the air and the GSHX as the heat source. Based on previous experimental results, a model of the HHP was developed. This model was then used with different borehole GSHX sizes and compared to a pure air source and a conventional ground source heat pump. They found that a significant reduction of the borehole dimensioning to 50 % showed only minor reductions in annual efficiency compared to a conventional ground source heat pump (-11 %), while improving the efficiency compared to the air source heat pump system (+26 %).

1.3. Research gap and scope

HHPs currently focus on utilizing one heat source at a time. However, utilizing both heat sources in parallel operation can provide significant flexibility to the heating system: while it is relatively simple to reduce the energetic load on a GSHX by reducing the heating load during comparatively high ambient temperatures by switching to air source operation (ASO), the peak load still requires a large heat exchanger area. This research aims at investigating the potential on efficiency and GSHX sizing by including parallel operation of both heat sources into a HHP by utilizing two compressors compared to conventional ground source heat pumps (GSHP).

This study focuses on building a model of a HHP which can not only switch between utilization of either heat source, but also allows parallel operation of both heat sources. An air as well as a ground source is used. The HHP was developed and tested experimentally in [9]. This paper aims at (a) developing a model based on this investigation including an operation mode controller for the single heat source operations as well as the parallel operation of both heat sources, and (b) an annual simulation to determine the effect on the annual efficiency, the total energy extracted from the GSHX and the heating capacity the GSHX needs to provide. By this, the energetic advantages of parallel operation are evaluated.

2. Methodology

The overall method of this paper includes the development of a black box model for the HHP including both the single source operations with the air source (ASO) and the ground source (ground source operation; GSO) as well as the parallel operation (PO). The experimental investigation in [9] provides the necessary data. This model is then implemented into an annual simulation with weather data, soil temperatures and a building heating load.

To evaluate the annual efficiency, the seasonal performance factor (SPF) is used with the cumulative energies for the heat Q_{heat} and the electricity E_{el} over the whole year:

$$\mathrm{SPF} = \frac{Q_{heat}}{E_{el}} = \frac{\sum \dot{Q}_{heat} * dt}{\sum P_{el} * dt} \tag{2}$$

The HHP model needs to yield the heating load $\dot{Q}_{heat}$ as well as the necessary electrical power P_{el} for each simulation time step dt. These values are also required for the evaluation of the energetic and power load on the GSHX. The extracted energy over a whole year E_{GSHX} can be calculated by evaluating the GSO and the corresponding difference between the heating capacity $\dot{Q}_{heat,\mathrm{GSO}}$ and the electrical power $P_{el,\mathrm{GSO}}$, also summed up over the simulation time steps dt. The energy extracted during PO is included here, since PO is assumed to be a combination of full power GSO and additional ASO.

$$E_{\mathrm{GSHX}} = \sum (\dot{Q}_{heat,\mathrm{GSO}} - P_{el,\mathrm{GSO}})\, dt \tag{3}$$

The maximum power load on the GSHX $\dot{Q}_{\mathrm{GSHX,max}}$ can be evaluated by finding the maximum of the aforementioned difference between the vectorial values of the heating capacity $\dot{Q}_{heat,\mathrm{GSO}}$ and the electrical power $P_{el,\mathrm{GSO}}$ during GSO:

$$\dot{Q}_{\mathrm{GSHX,max}} = max(\dot{Q}_{heat,\mathrm{GSO}} - P_{el,\mathrm{GSO}}) \tag{4}$$

2.1. Development of the black box model

The model type of the heat pump was chosen to be a black box model to limit the computing time. For each operation mode one performance map was developed based on the measurements in [9]. These measurements described the heating and electrical powers ($\dot{Q}_{heat,\mathrm{GSO}}$ and $P_{el,\mathrm{GSO}}$ respectively) depending on boundary conditions like ambient temperature T_a, source inlet temperature $T_{\mathrm{so,GSO}}$ and sink outlet temperature T_{si} based on [10]. The detailed control of the HHP model described below was then realized within the simulation model.

The heating controller switched between the operation modes depending on the ambient temperature. The inverter frequency f_{inverter} resulted in a non-linear behavior of the heating and electrical power. This was included into the model. The range allowed for the inverter was $0 - 100$ %.

Two bivalence points were defined: bivalence point 1 T_{biv1} is the temperature, when the HHP switches from ASO to GSO and vice versa. Bivalence point 2 T_{biv2} is the temperature, when the HHP switches from GSO to PO and vice versa. A heating threshold temperature T_{thr} was implemented, at which the general operation of the HHP switched on and off depending on the moving mean ambient temperature $T_{a,\mathrm{mean}}$ over the last seven days. Figure 1 shows the general structure of the decision tree to determine the operation mode.

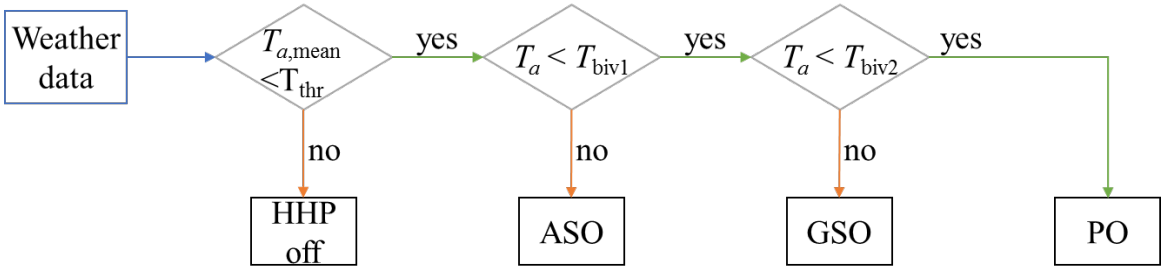

Fig. 1: Decision tree of the HHP model to derive the operation mode. Each check includes a hysteresis.

The GSO model had the inputs of source temperature from the GSHX, the outlet temperature of the heating system and the inverter frequency. The performance map along with the inverter correction factor then determined the output heating capacity and the electrical power.

The ASO model worked similar, except that the input for the source was the ambient temperature.

The PO was the combination of both operation modes. In this work, below the bivalence point 2 T_{biv2}, the GSO continued at maximum inverter frequency. Additionally, the ASO was added to the GSO at maximum inverter frequency: the inverter frequency fed into the PO model then only changed the frequency of the ASO. Both source temperatures for the ground source and the ambient temperature were needed for PO, since both compressors are running in this operation mode.

2.2. Description of the annual simulation

This HHP model was then implemented into an annual simulation. The general scheme of the annual simulation is shown in Figure 2. The input data consisted of a weather data set for Ingolstadt, Germany, in the format of a test reference year [11]. For the GSO, the source temperature was derived from an undisturbed ground temperature model. This ground temperature model was based on approaches for seasonal temperature variations in the ground [12, 13]. A horizontal GSHX was used, buried in a depth of 1.5 m. Additionally, for the heat transfer to the brine cycle, a temperature difference of 3 K was assumed below this undisturbed ground temperature for the source temperature.

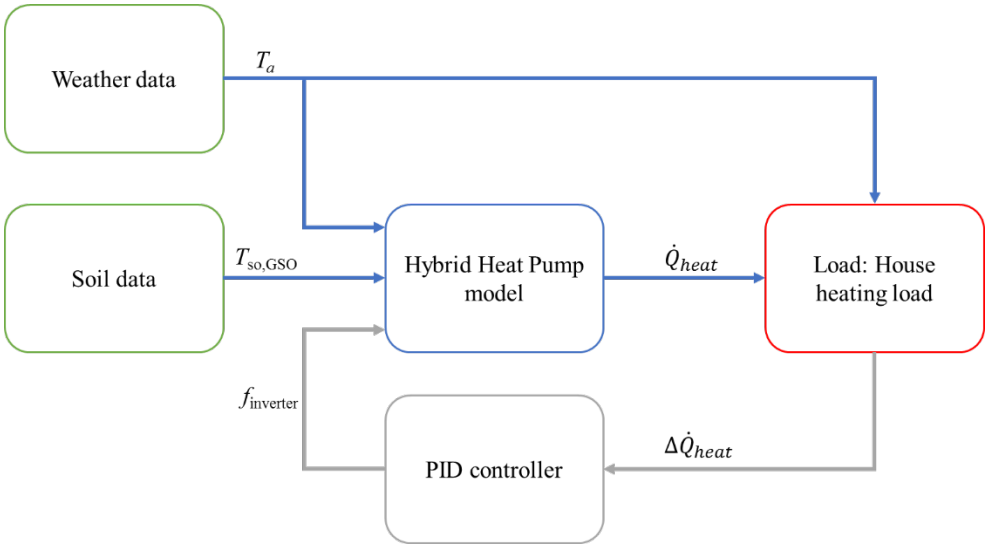

Fig. 2: Scheme of the annual simulation for the HHP. Sources (green) and load (red) are integrated as the periphery for the HHP model, a PID controller (grey) is used for determination of the necessary inverter frequency.

The load was described by a simple linear house heating load $\dot{Q}_{heat,\mathrm{set}}$ dependent on the ambient temperature. The conditions were:

- $\dot{Q}_{heat,\mathrm{set}}(T_a = 20\ °\mathrm{C}) = 0$ kW, assuming a target room temperature of 20 °C and no internal gains.
- $\dot{Q}_{heat,\mathrm{set}}(T_a = -20\ °\mathrm{C}) = 10$ kW, assuming maximum load at −20 °C.

This led to the following calculation for the necessary heating load of the house dependent on the ambient temperature:

$$\dot{Q}_{heat,\mathrm{set}} = -0.25\ \frac{\mathrm{kW}}{\mathrm{K}} * T_a + 5\ \mathrm{kW} \tag{5}$$

Then PID controller compared the necessary heating load with the delivered heating load delivered by the HHP $\dot{Q}_{heat}$. It then changed the frequency accordingly to minimize the error $\Delta\dot{Q}_{heat}$. It is important to note, that only one single inverter frequency is varied at a time: for the active compressor during ASO and GSO and during PO, the GSO compressor worked at maximum frequency and only the ASO compressor was controlled by the PID controller signal. The PID controller operated only with a proportional gain P = 0.5 and an integral

gain I = 0.1. The derivative gain was found to be not necessary. Also, the PID controller reset with every operation change of the HHP model due to non-linear behavior.

Since the heating system was designed around a buffer storage tank, the sink temperature of the HHP was assumed to be constant $T_{\mathrm{si}} = 35$ °C. Only space heating on floor heating temperature levels was considered. Bivalence point 1 was chosen to be $T_{\mathrm{biv1}} = 4$ °C with a hysteresis of ±1 K. Each change of operation mode leads to one compressor start (either the GSO compressor switches off and the ASO compressor switches on or vice versa), which should be limited to avoid damaging the compressor. Bivalence point 2 was set to be $T_{\mathrm{biv2}} = -3$ °C. A lower hysteresis of +1 K was chosen, because only the change from GSO to PO leads to one compressor start (from PO to GSO only deactivates the ASO compressor). This indicates that repeated switching between GSO and PO is half as harmful to the number of compressor starts compared to a switching between ASO and GSO. The heating threshold temperature was $T_{\mathrm{thr}} = 12$ °C with a hysteresis of +1 K.

The output data consisted of the current operation mode (ASO, GSO or PO) including the inverter frequency, the weather and soil data and the HHP output data for the heating and electrical power.

3. Annual simulation results

3.1. Analysis of the HHP black box model within the simulation

The main inputs of the simulation are shown in Figure 3(a). While the ambient temperature fluctuated significantly on a short time frame, the moving average ambient temperature showed a much smoother behavior. This led to a clearer distinction of whether heating is necessary or not, which finally resulted in less on-off cycles. This clear separation of no operation in summer time due to dependency of the mean ambient temperature can be observed in Figure 3(b). The inverter frequency was normalized to a relative value of its maximum. During summer time, the relative inverter frequency remained at zero, which here means the heat pump is switched off. Also shown in Figure 3(a) is the source temperature of the GSHX. The large thermal

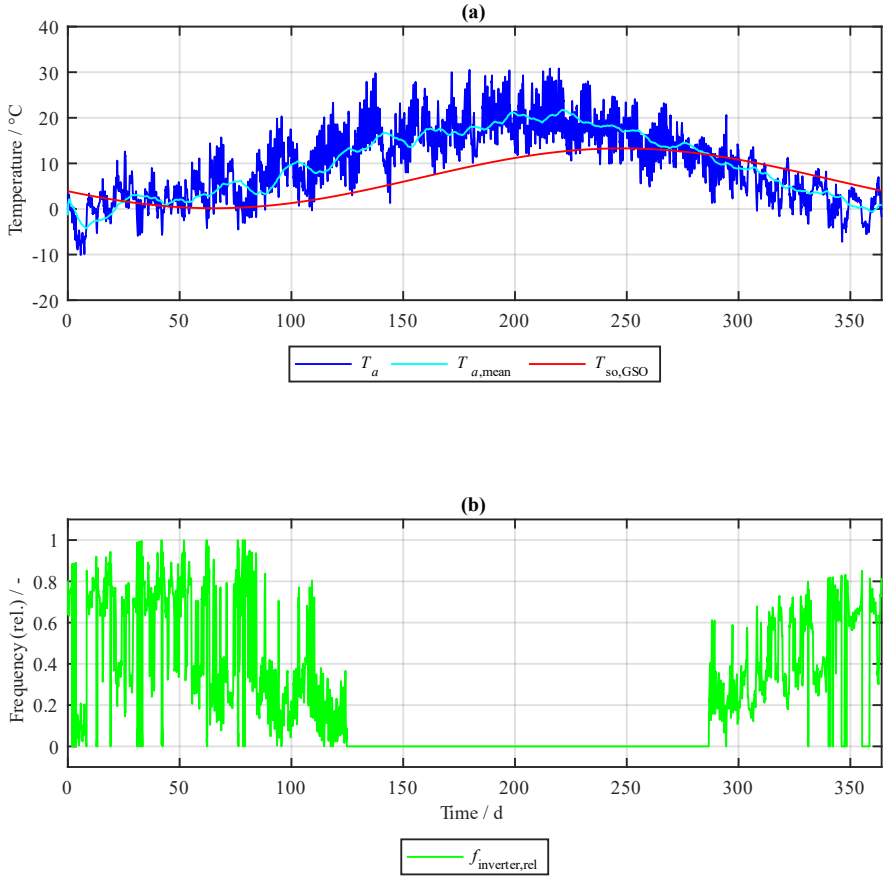

Fig. 3: Overview of the annual operation of the HHP. (a) shows the input parameters of the ambient temperature T_a, the moving mean ambient temperature over 7 days $T_{a,\mathrm{mean}}$ and the source temperature of the GSHX $T_{\mathrm{so,GSO}}$. (b) shows the relative inverter frequency $f_{\mathrm{inverter,rel}}$.

inertia of the ground leads to smaller amplitudes and a phase shift. It can be seen that especially in the last weeks of the year, the ground source temperature was notably higher than the ambient temperature, leading to a higher source temperature for the refrigeration cycle and therefore more efficient GSO compared to ASO. At the same time, however, in spring it seemed to be more beneficial to let the HHP run in ASO mode due to a cooled GSHX. A flexible bivalence point 1 depending on the ground source temperature should be analyzed, even though the increasing ambient temperatures indicate lower heating loads and therefore less impact on the annual efficiency. More detailed GSHX models are needed to verify this behavior of the slowly changing ground source temperatures which could impact the dependencies used for the bivalence points.

Next, the switching around the bivalence points 1 and 2 was analyzed exemplarily. In Figure 4, the ambient temperature during the last two weeks of the year can be observed. Additionally, the state of the GSO is shown: at 1, the state is ON, so GSO is active. At 0, GSO is off/inactive. Around day 356, the ambient temperature dropped below $T_{\mathrm{biv2}} = -3\ °\mathrm{C}$ and GSO was replaced with PO. For this, the GSO operates at maximum inverter frequency and ASO is added to cover the necessary heating load. This remained the case until the ambient temperature rose above the bivalence point including the hysteresis $T_{\mathrm{biv2}} + 1\ \mathrm{K} = -2\ °\mathrm{C}$ about two days later. Then, GSO reactivated instead of PO. GSO remained active until the ambient temperature increased above bivalence point 1 including hysteresis $T_{\mathrm{biv1}} + 1\ \mathrm{K} = 5\ °\mathrm{C}$ on day 362. GSO deactivated and ASO started instead until the ambient temperature decreased below the bivalence point 1 including hysteresis one day later $T_{\mathrm{biv1}} - 1\ \mathrm{K} = 3\ °\mathrm{C}$. The switching was operative and worked according to the rules.

The inverter frequency was controlled as expected. However, during PO the low inverter frequency indicates that PO was not really needed yet and the bivalence point 2 was set too high for these weeks. During GSO – when the state of the GSO is on –, the relative inverter frequency varied to match the heating capacity of the HHP to the necessary heating capacity defined by equation (6). The same was the case during ASO from day 362 to 363. One notable difference was the lower relative inverter frequency during ASO compared to GSO. The reason for this was a higher heating capacity by the ASO compressor than the GSO compressor's capacity. This led to a lower necessary inverter frequency to cover the load, which in turn led to the non-linear jump in the inverter frequency. The PID controller was reset during the operation mode change and therefore reacted quickly to minimize the heating capacity difference to the necessary heating load.

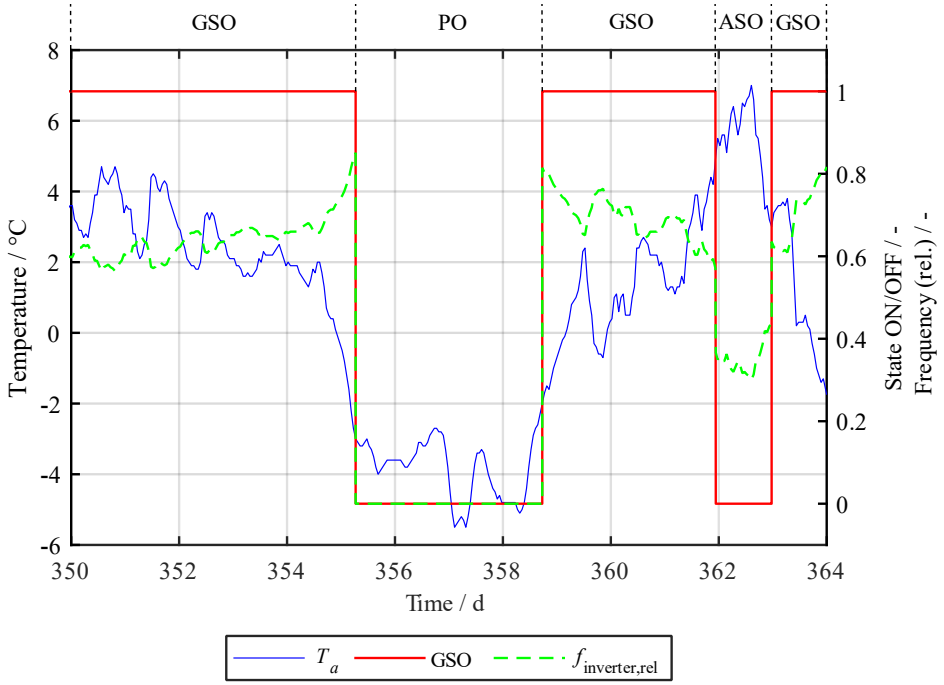

Fig. 4: Example of the switching procedure for both bivalence points 1 and 2 during the last two weeks of the year. For visibility, only the GSO is shown switching on and off.

Non-intuitive was the relative inverter frequency during PO from day 356 to 359. The value during this time was zero, indicating a switched-off air source compressor, since the ground source compressor was supposed to run at full inverter frequency during this operation mode. The explanation is, that the GSO was still able to cover the necessary heating load below maximum inverter frequency. This is an indicator, that the parallel operation was activated at too high temperatures when it was not yet necessary. However, at earlier

stages during the year, this was not the case: since the heating capacity of the GSO depends on the ground source temperature as well, the heating capacity of the GSO is reduced during late winter/early spring as shown in the GSHX source temperature in Figure 3. During times of still high source temperatures during GSO in late autumn/early winter, GSO could therefore provide enough heating capacity on its own and PO was activated with a deactivated air source compressor.

Figure 5 shows the operation modes (here: GSO and PO) during the first week of the year. Here, during PO starting at day 4 the frequency actually varied up to around 20 %, indicating that the GSO cannot cover the full heating load anymore due to a lower source temperature level of the GSHX. In this week PO was therefore necessary. This indicated that a flexible bivalence point 2 is required for proper coverage of the necessary heating load.

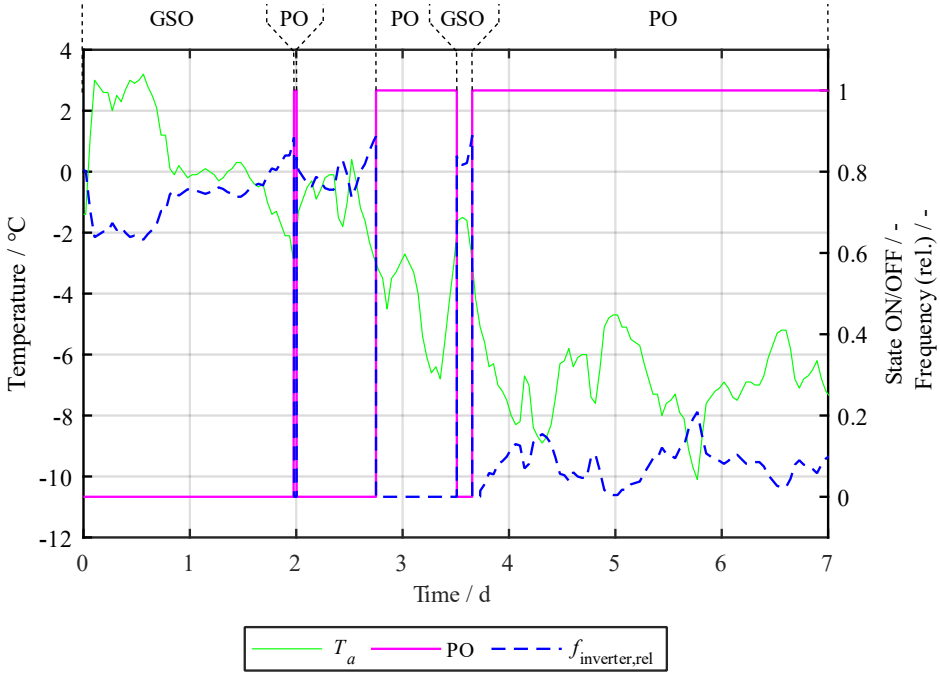

Fig. 5: Example of the relative inverter frequency at certain operation modes (ASO, GSO, PO) during the last two weeks of the year.

3.2. Effects of PO on annual efficiency and the GSHX

Still, the HHP showed an annual efficiency calculated using equation (2) of SPF = 4.37 for floor heating operation. The total delivered heating energy was $E_{heat} = 18.9$ MWh and the electrical energy $E_{el} = 4.3$ MWh. The energy extracted from the soil is the sum of the energy extracted during GSO and the GSHX energy extracted during PO. Equation (3) yielded $E_{\text{GSHX}} = 8.9$ MWh, which is a fraction equal to about 47.1 % of the delivered heating energy. The remaining energy was taken from the ambient air:

$$E_{\text{air}} = E_{heat} - E_{\text{GSHX}} - E_{el} = 5.7\ MWh \tag{7}$$

Using the same periphery (source and load), a conventional GSHP yielded an annual efficiency of $\text{SPF}_{\text{GSHP}} = 4.27$ and extracted heat energy from the GSHX of $E_{\text{GSHX,GSHP}} = 14.4$ MWh. The HHP showed improvements on both values: The SPF increased by about 2 %, the energy extracted from the soil to about 62 %. The bivalence points need to be examined further to not only allow flexibility as mentioned before, but also to analyze further reduction in GSHX size.

The heating capacity necessary by the GSHX was evaluated as well. The maximum difference per time step between the heating capacity $\dot{Q}_{heat}$ and the electrical power P_{el} resulted in $\dot{Q}_{\text{GSHX,max}} = 4.5$ kW. The comparison with a GSHP led to $\dot{Q}_{\text{GSHX,max,GSHP}} = 5.6$ kW. This was a relatively small difference of about 1 kW (or down to almost 80 %), indicating a limited power reduction due to PO of the HHP. This power reduction should be evaluated further: with an increased necessary heating load during PO, this effect should

be more distinct, because further air source power needs to be added to cover the heating load, while the power on the GSHX remains the same.

Lastly, the PID controller was operating properly. The mean error of heating load and necessary heating load over the whole year was $\Delta\dot{Q}_{heat,\mathrm{mean}} = -2.9\ \mathrm{W}$. So even though the PO mode often led to significant heating capacity differences when it was activated at too high ambient temperatures, the mean error heating capacity difference over the whole year was reasonably small.

3.3. Discussion of the results

The decision tree for the operation mode determination worked as intended: depending on the ambient temperature, one operation mode was active to cover the necessary heating load. Appropriate hysteresis's prevented repeated switching between the operation modes, which in turn would lead to an increase in compressor starts. The $\mathrm{SPF} = 4.37$ was comparable to market available GSHPs and the heat extracted from the soil $E_{\mathrm{GSHX}} = 8.9\ \mathrm{MWh}$ was reduced to about 62 % compared to conventional ground source heat pumps.

This can allow a reduction in size of the GSHX. However, the potential needs to be further evaluated with varying bivalence points as described in chapter 3.1 and also varying sink temperature levels with radiant heaters and/or without buffer storage.

Also, the inverter frequency control was working properly, covering the necessary heating load over the whole year at a small error. Especially during ASO and GSO, the PID controller worked well, while it struggled matching the heating load during PO. However, this was an issue of the bivalence point 2, not the PID controller. Also, in practice most inverters do not allow lower frequencies below about 25 %, which needs to be included in future simulations.

There are several steps which need to be improved in the simulation to enable further more detailed evaluations: first, the model of the PO is a simple combination of the single source operations. Since both operation modes share one condenser heat exchanger (see the interconnection in [9]), this is a simplification. The PO needs to be examined more closely in the laboratory to determine a proper PO model. Also, allowing a variation of the GSO inverter frequency during PO can add another level of flexibility: even at higher ambient temperatures, when GSO is more efficient than ASO but PO is not strictly necessary yet, running both inverters in part-load can reduce the energy extracted from the GSHX without a large influence on the efficiency.

The bivalence points are the second necessity: during the annual simulation, the ASO was often not used to its full extend. It is even possible that the annual efficiency increases by decreasing bivalence point 1. Also, bivalence point 2 needs dependencies to allow a more beneficial PO. Dependencies on the ground source temperature, building or buffer storage temperature or on the year's month are options for further examinations.

The periphery for the annual simulation is currently still simplified. The load is a linear heating load, which requires not the highest heating capacities possible by the HHP. Domestic hot water is not included yet, which also makes the heating controller more complex. The sources need to be modelled more in detail to show more complex behavior. Especially the GSHX was simplified in this work. Dynamic behavior of heat extraction and regeneration could therefore not yet be simulated.

Further operation modes possible to the interconnection [9] need to be implemented. Some of these requirements, especially active regeneration, need more detailed GSHX models to show their potential.

4. Conclusion

The interconnection of the HHP allows for an increased efficiency compared to conventional GSHPs. The increase in SPF from 4.27 for the GSHP to 4.37 for the HHP is an increase by only about 2 %, which is marginal. The HHP also reduced the extracted energy from the GSHX to about 62 %. PO specifically reduced the maximum heating load to about 80 %. These findings indicate a significant reduction possibility in dimensioning of the GSHX, while the increase in efficiency is marginal.

Further improvements of the simulation need to be applied. Most important are detailed heat source and heat sink models. The HHP model needs to include non-linear inverter frequency influence and limits as well as comprehensive PO modelling. On the controller side, especially the bivalence points – when to switch between ASO, GSO and PO – need to be examined and optimized.

Acknowledgements

The Project “Hybrid Heat Pump+” is supported by the Federal Ministry for Economic Affairs and Climate Action (BMWK) on the basis of a decision by the German Bundestag.

References

[1] Bundesverband Wärmepumpe e.V., "www.waermepumpe.de," BWP Marketing & Service GmbH, 20 January 2022. [Online]. Available: https://www.waermepumpe.de/presse/pressemitteilungen/details/starkes-wachstum-im-waermepumpenmarkt/. [Accessed 20 October 2022].

[2] Agora Energiewende, "Wärmewende 2030 - Schlüsseltechnologien zur Erreichung der mittel- und langfristigen Klimaschutzziele im Gebäudesektor," Berlin, 2017.

[3] I. Dincer, "Energy and Exergy Efficiencies," in *Comprehensive Energy Systems*, Oshawa, ON, Canada, Elsevier, 2018, pp. 265-339.

[4] John Cantor Heat Pumps, "https://heatpumps.co.uk," n.d.. [Online]. Available: https://heatpumps.co.uk/heat-pump-information-without-the-hype/what-is-the-cop/. [Accessed 01 September 2022].

[5] C. Naldi, E. Zanchini and G. L. Morini, "A method for the choice of the optimal balance-point temperature of air-to water heat pumps for heating," *Sustainable Cities and Society,* vol. 12, pp. 85-91, 01 July 2014.

[6] K. Allaerts, M. Coomans and R. Salenbien, "Hybrid ground-source heat pump system with active air source regeneration," *Energy Conversion and Management,* vol. 90, pp. 230-237, 04 November 2014.

[7] M. Cannistraro, E. Mainardi and M. Bottarelli, "Testing a dual-source heat pump," *Mathematical Modelling of Engineering Problems,* vol. 5, pp. 205-210, 2018.

[8] M. Dongellini, C. Naldi, C. Natale and G. L. Morini, "Modelling of a dual-source heat pump with Matlab/Simulink and Almabuild/Carnot," in *Simulation assisted design and optimisation of heat pumps and heat pump applications - from refrigerant cycle simulation to building and district heating integration*, Innsbruck, 2022.

[9] T. Reum, T. Summ, M. Ehrenwirth and T. Schrag, "Experimental Investigation of a Novel Hybrid Heat Pump," *Submitted to EuroSun 2022: ISES and IEA SHC Conference on Solar Energy for Buildings and Industry,* 2022.

[10] DIN e.V., DIN EN 14511:2019-07, Air conditioners, liquid chilling packages and heat pumps for space heating and cooling and process chillers, with electrically driven compressors, Berlin: Beuth Verlag GmbH, 2019.

[11] Deutscher Wetterdienst, "Testreferenzjahre (TRY)," 2017. [Online]. Available: https://www.dwd.de/DE/leistungen/testreferenzjahre/testreferenzjahre.html. [Accessed 25 October 2022].

[12] H. D. Baehr and K. Stephan, Wärme- und Stoffübertragung, Heidelberg: Springer-Verlag, 2006.

[13] V. Wesselak and T. Schabbach, Regenerative Energietechnik, Heidelberg: Springer-Verlag, 2009.